Supporting Information

Chestnut-Like TiO_2@α-Fe_2O_3 Core-Shell Nanostructures with Abundant Interfaces for Efficient and Ultralong Life Lithium-Ion Storage

Jingling Yang,[†] *Qili Wu,*[†] *Xianfeng Yang,*[‡] *Shiman He,*[†] *Javid Khan,*[†] *Yuying Meng,*[†] *Xiuming Zhu,*[†] *Shengfu Tong,**[†] *Mingmei Wu**[†]

[†]MOE Key Laboratory of Bioinorganic and Synthetic Chemistry, Key Laboratory of Environment and Energy Chemistry of Guangdong Higher Education Institutes, School of Chemistry, Sun Yat-Sen University, Guangzhou 510275, P. R. China

[‡]Analytical and Testing Center, South China University of Technology, Guangzhou 510640, P. R. China.

Corresponding authors:

*E-mail: tongshf@mail.sysu.edu.cn

*E-mail: ceswmm@mail.sysu.edu.cn

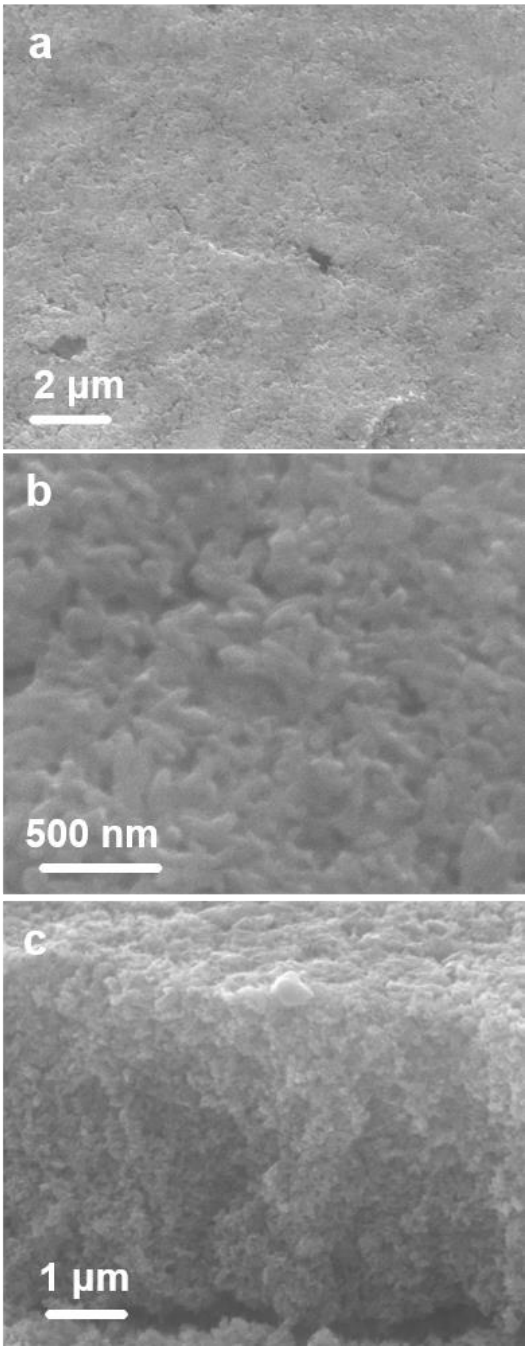

Figure S1. Low-magnification (a) enlarged (b) and cross-sectional (c) SEM images of α-Fe_2O_3 nanorods on Ti foil.

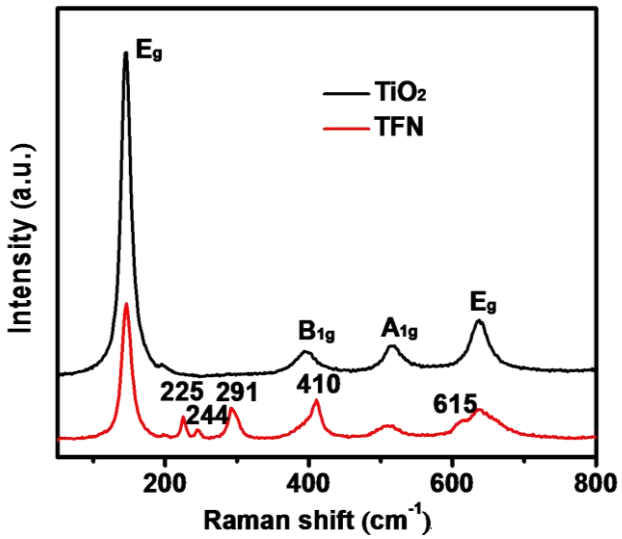

Figure S2. Raman spectra of the as-synthesized TiO_2 and TFN.

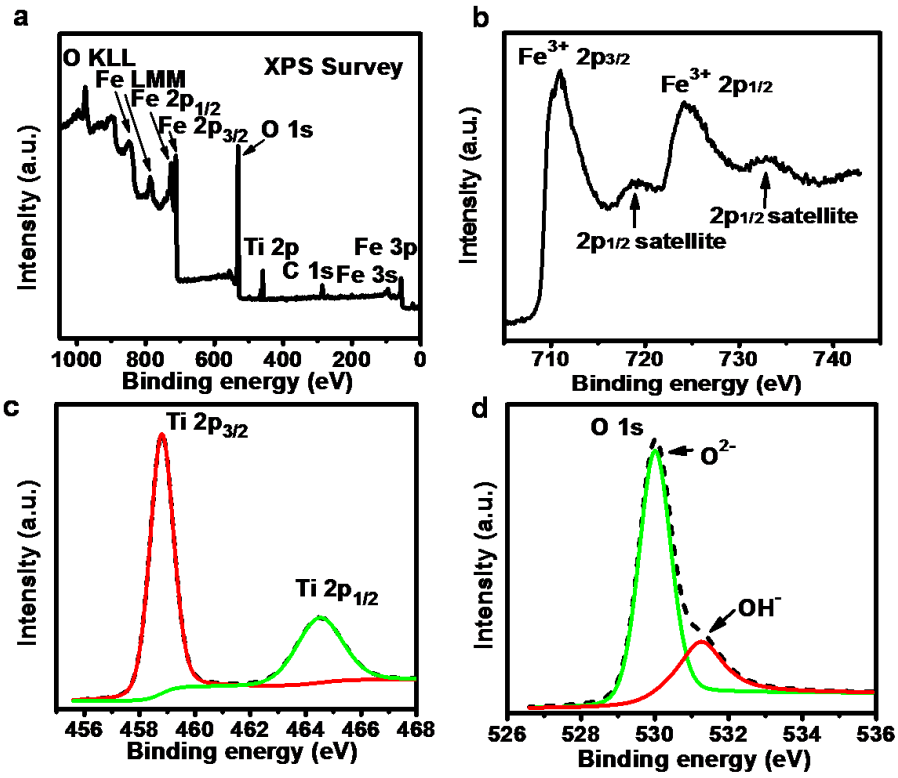

Figure S3. XPS spectra of TFN composite. (a) Survey scans, (b) Fe 2p peaks, (c) Ti 2p peaks and (d) O 1s.

The surface chemical compositions and the valence states of TFN were revealed by Raman (Figure S2) and XPS (Figure S3), respectively. The Raman spectrum recorded from Figure S2 exhibits nine intense bands located at 146, 225, 244, 291, 393, 410, 504, 615 and 635 cm^{-1}. The bands at 146, 393, 504 and 635 cm^{-1} match anatase TiO_2,[1] while the other bands agree well with the A_{1g}, E_g, E_g, E_g and E_g vibrational modes of rhombohedral Fe_2O_3,[2] which further provides the evidence for the co-existence of crystalline TiO_2 and α-Fe_2O_3. The presence of O 1s, Ti 2p and Fe 2p in the sample was checked by XPS (Figure S3). In Figure S3b, Fe $2p_{3/2}$ and Fe $2p_{1/2}$ peak at 711.0 eV and 724.2 eV can be assigned to Fe (III), which confirm the formation of Fe_2O_3. Furthermore, the peaks at 458.8 eV and 464.5 eV in the Ti 2p spectrum can be

assigned to the $2p_{3/2}$ and $2p_{1/2}$ core levels of a normal state of Ti (IV) in the anatase TiO_2 (Figure S3c).[3] The peaks (Figure S3d) of the O 1s spectrum are resolved into two components, at 530.0 and 531.3 eV, respectively. The low binding energy component observed at 530.0 eV is attributed to the O^{2-} forming oxide with titanium and iron elements, the latter peaks are assigned to OH^-.[4, 5]

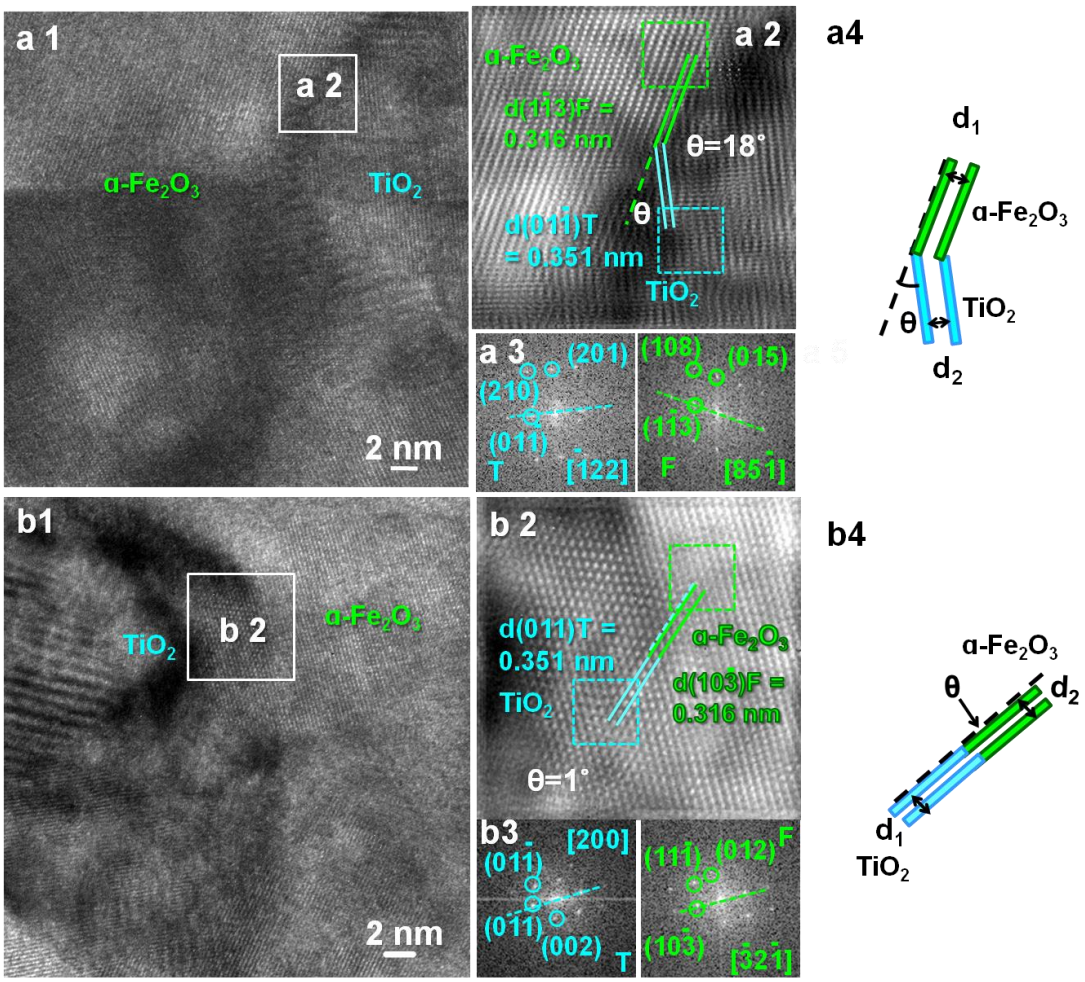

Figure S4. (a1, b1) High resolution TEM images of two random areas of TFN after the 50th cycle. (a2, b2) High resolution TEM images magnified from the area outlined by the white square in panel (a1, b1), respectively. (a3, b3) Corresponding fast Fourier Transformation pattern from the area outlined by green and blue dotted squares in panel (a2, b2), respectively. (a4, b4) Schematic diagrams of the interfaces match between TiO_2 and α-Fe_2O_3 correspond to (a2, b2). "T" and "F" in the pictures represent α-Fe_2O_3 and anatase TiO_2 phases, respectively.

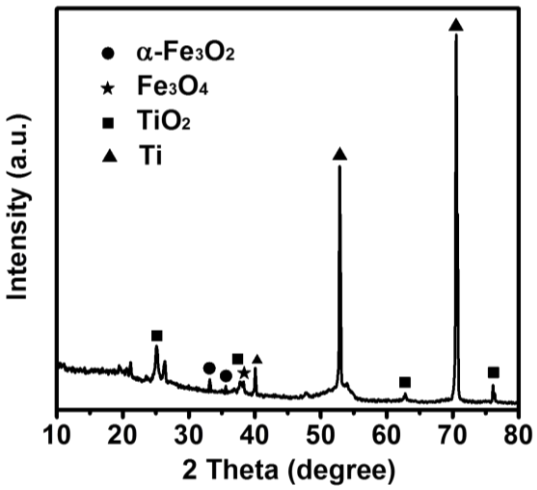

Figure S5. XRD pattern of the core-shell TFN electrode after 50 cycles.

The boundary structures of TFN electrode after 50 cycles were revealed by HRTEM and XRD. The TEM images in Figure S4 and XRD patterns in Figure S5 show that even after the 50th cycle, abundant interfaces between anatase TiO_2 and hematite α-Fe_2O_3 were also observed. For instance, Figure S4a-b show two segments of TFN after the 50th cycle. The HRTEM micrograph of interfacial region magnified from Figure S4a2 and b2 displays two distinctive interface made of anatase TiO_2 $(01\bar{1})$ plane and α-Fe_2O_3 $(1\bar{1}3)$ plane with a deviation angle of 18^o, as well as anatase TiO_2 (011) plane and α-Fe_2O_3 $(01\bar{3})$ plane with a deviation angle of 1^o, respectively. The corresponding FFT patterns taken from α-Fe_2O_3 and TiO_2, while outlined by the dotted square further confirms these lattice-matched interface (Figure S4a3 and b3). The XRD pattern also confirmed the co-existence of TiO_2 and α-Fe_2O_3 in TFN after the 50th cycle (Figure S5), while the signals of Fe_3O_4 (JCPDS card no. 65-3107) were also observed. This was attributed to the lithium storage mechanism in the α-Fe_2O_3 primarily accompanied with the redox processes ($Fe^{3+} \leftrightarrow Fe^{2+}/Fe^0$). Thus, these results confirmed that the TiO_2@α-Fe_2O_3 (TFN) after the 50th cycle can still maintain the abundant interfaces structure.

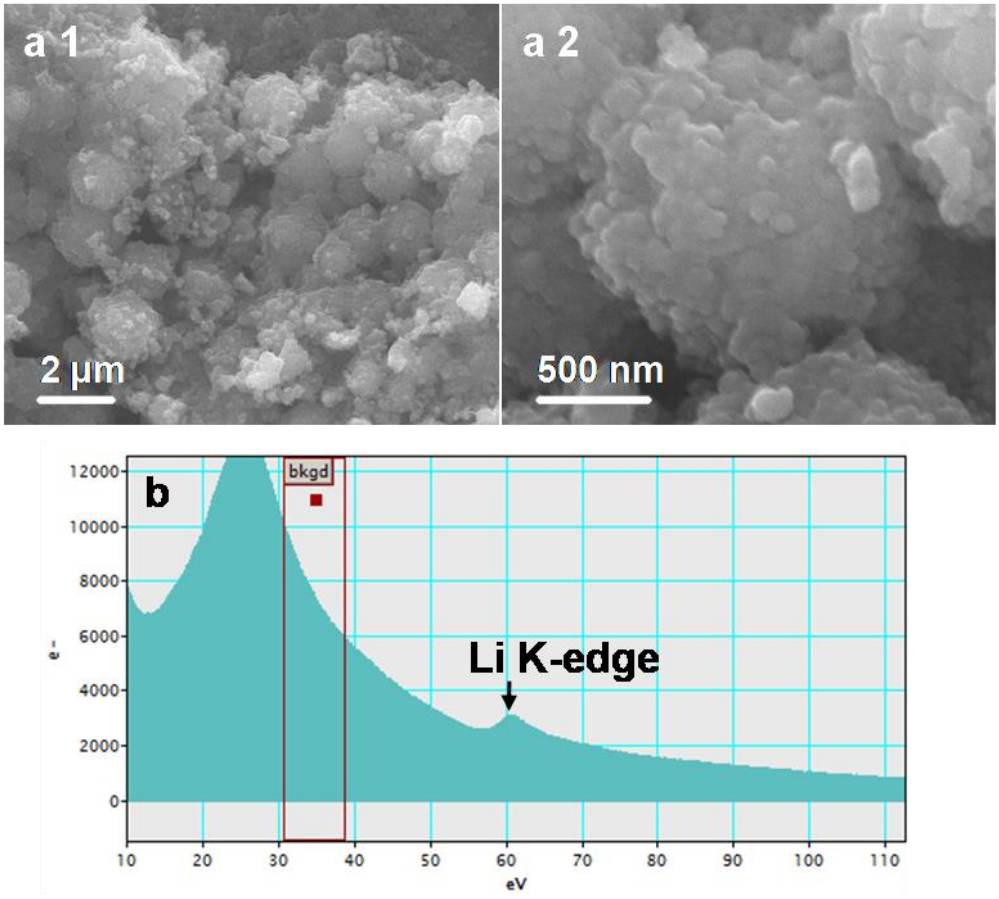

Figure S6. Low (a1) and high-magnification (a2) SEM images of TFN after 200 cycles. (b) EELS of Li element in TFN after 200 cycles.

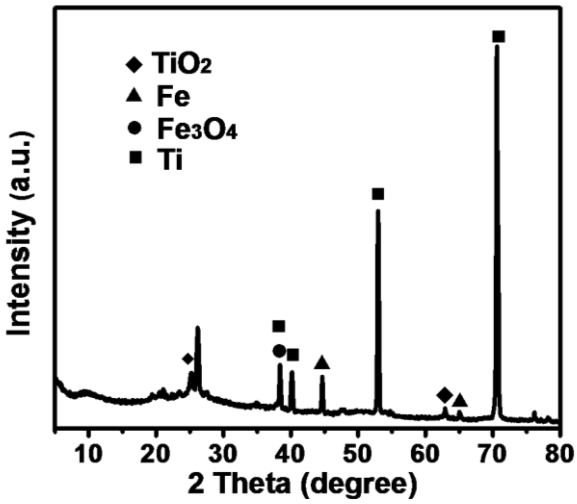

Figure S7. XRD pattern of the core-shell TFN electrode after 1000 cycles.

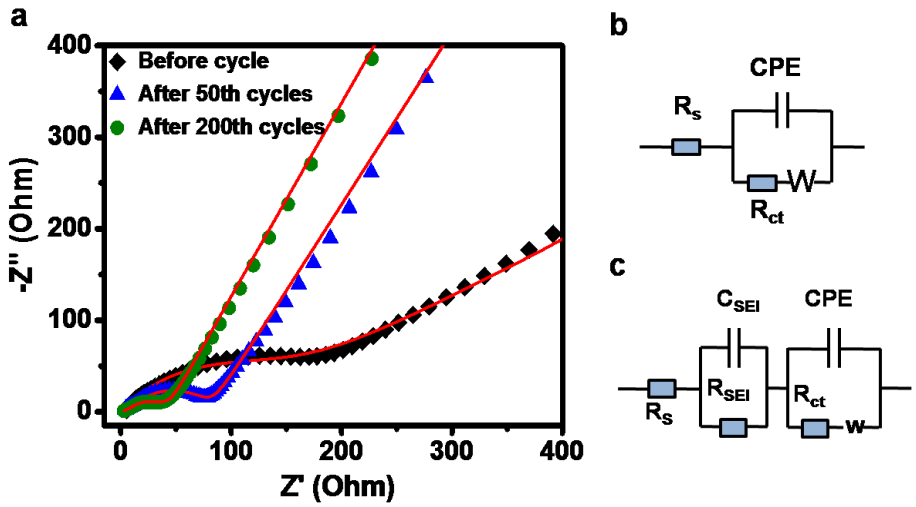

Figure S8. (a) Nyquist plots for the TFN electrodes, freshly assembled (black), experienced 50 (blue) and 200 cycles (green), correspondingly. (b) The equivalent circuit model of the freshly assembled TFN electrode (black dot line in Figure S6a). (c) The equivalent circuit model of the TFN electrode experienced discharge-recharge cycles (blue and green dot line in Figure S8a).

References

（1） Yang, J.; Wu, Q.; He, S.; Yan, J.; Shi, J.; Chen, J.; Wu, M.; Yang, X. Completely <001> Oriented Anatase TiO_2 Nanoarrays: Topotactic growth and Orientation-Related Efficient Photocatalysis. *Nanoscale* **2015**, *7,* 13888-13897.

（2） Qin, L.; Pan, X.; Wang, L.; Sun, X.; Zhang, G.; Guo, X. Facile Preparation of Mesoporous TiO_2(B) Nanowires with Well-Dispersed Fe_2O_3 Nanoparticles and their Photochemical Catalytic Behavior. *Appl. Catal. B: Environ.* **2014**, *150-151,* 544-553.

（3） Yamashita, T.; Hayes, P. Analysis of XPS Spectra of Fe^{2+} and Fe^{3+} Ions in Oxide Materials. *Appl. Surf. Sci.* **2008**, *254,* 2441-2449.

（4） Bhargava, G.; Gouzman, I.; Chun, C. M.; Ramanarayanan, T. A.; Bernasek, S. L. Characterization of the “Native” Surface Thin Film on Pure Polycrystalline Iron: A High Resolution XPS and TEM Study. *Appl. Surf. Sci.* **2007**, *253,* 4322-4329.

（5） Pradhan, G. K.; Martha, S.; Parida, K. M. Synthesis of Multifunctional Nanostructured Zinc-iron Mixed Oxide Photocatalyst by a Simple Solution-Combustion Technique. *ACS Appl. Mater. Interfaces,* **2011**, *4,* 707-713.